

The Eurasia Proceedings of Science, Technology, Engineering & Mathematics (EPSTEM), 2022

Volume 18, Pages 28-36

ICBASSET 2022: International Conference on Basic Sciences, Engineering and Technology

Development of Two-Dimensional Thermal Analysis Code for the Analysis of 3D Printed PLA Parts

Buryan APACOGU-TURAN

İstanbul Technical University

Kadir KIRKKOPRU

İstanbul Technical University

Abstract: Fused Deposition Modelling is one of the main 3D printing methods to manufacture plastic parts. The strength of the printed part by FDM is dependent on polymer diffusion between printed layers. The polymer diffusion between two neighboring layers occur not only during the extrusion of the hot top layer, but also during the production of consecutive layers due to thermal conduction. The heat diffusion from upper layers enhances the curing of polymers, which consequently affects the strength of the part. Therefore, the history of the temperature variations - curing time and curing temperature - should be analyzed to predict the strength of the part. The goal of this study is to develop a two-dimensional transient thermal analysis solver for the investigation of time-dependent thermal changes during the printing process. This solver is developed with the use of finite difference method employed under implicit scheme. The transient temperature pattern is qualitatively compatible to the experimental results in literature. The solver can be utilized for further thermal analyses to correlate temperature, polymer diffusion and strength with the inclusion of deposition path in the third dimension.

Keywords: Heat transfer, Simulation, Computational methods, Additive manufacturing, Polymers

Introduction

Additive manufacturing technologies have been developing in recent years. In three-dimensional printers, which can be of different types for different types of materials, Fused-Deposition Modeling (FDM) is widely used to produce plastic parts. In this method, plastic filaments are melted through a moving nozzle and laid in layers on a surface. The polymer structures inside the plastic layers provide this adhesion by diffusing from one layer to the next (Wool & O'Connor, 1981).

Thanks to this approach, rapid prototyping can be performed with low costs. When compared to traditional manufacturing technologies such as CNC, it is seen that FDM method is a production method that consumes much less energy and generates much less waste (Faludi, Bayley, Boghal, & Iribarne, 2015). On the other hand; quality problems are observed in parts produced with FDM (Bikas, Stavropoulos, & Chryssolouris, 2016). The high durability of the part that comes out at the end of the production process depends on the completion of the diffusion of polymers (Bartolai, Simpson, & Xie, 2018). The ratio of the strength (σ_{weld}) of the part produced by FDM to the strength (σ_{∞}) of the bulk part with fully developed bonds gives the Bonding Degree (D_h) (Yang & Pitchumani, 2002):

$$D_h(t) = \frac{\sigma}{\sigma_{\infty}} \quad (1)$$

- This is an Open Access article distributed under the terms of the Creative Commons Attribution-Noncommercial 4.0 Unported License, permitting all non-commercial use, distribution, and reproduction in any medium, provided the original work is properly cited.

- Selection and peer-review under responsibility of the Organizing Committee of the Conference

© 2022 Published by ISRES Publishing: www.isres.org

According to Edward; a polymer is contained in a virtual tube where it does not interact with other polymers around it (Edward, 1988). The time required for the polymer to come out of this tube is called the reptation time (τ_{rep}). Materials that exceed the reptation time are able to form bonds that provide strength. According to Edward's Tube Theory; the shorter the reptation time, the faster the binding occurs. The reptation time is affected by the temperature of the polymer-polymer interlayer and the time-dependent variation of its temperature. The correlation showing this situation is as follows (Bartolai, Simpson, & Xie, 2018) :

$$\left| D_h(t) = \frac{\sigma_{weld}}{\sigma_{UTS}} \right. \quad (2)$$

In polymer-polymer interlayers that do not reach the reptation time, the durability (σ_{weld}) becomes lower. The welding time of the parts that cannot reach the reptation time is shown with t_{weld} . σ_{weld} is proportional to $(t_{weld})^{1/4}$ (Jud, Kausch, & Williams, 1981). With the help of this relation, the expression for the degree of bonding can be written in terms of times as follows:

$$\left| \frac{\sigma_{weld}}{\sigma_{UTS}} = \left(\frac{t_{weld}}{\tau_{rep}} \right)^{1/4} \right. \quad (3)$$

The main reason for quality problems is the variation of interlayer bond strength (polymer diffusion) depending on temperature and time-dependent changes in temperature (Yang & Pitchumani, 2002). In addition, the temperature in the interlayers and the history of temperature change affect the t_{weld} . For example; while the manufacturing process is at layer 30, how the temperature in layer 5 changes or rises above the glass transition temperature (T_g) will affect bonding. Hence, it is important to monitor the temperature of each layer during the production process. Time intervals above T_g at different layers should be examined for the estimation of bonding degree. It is expected that the layer with the shortest binding time will have the weakest point.

In an experimental study (Coogan & Kazmer, Bond and part strength in fused deposition modeling, 2017) it was observed that the strength of the upper layers was higher in the production scenario tested. It is stated that a comprehensive heat transfer analysis model and software is needed to predict which layer is the weakest in different scenarios. The authors in another study (Coogan & Kazmer, Healing simulation for bond strength prediction of FDM, 2017) modeled the top 2 layers by making 1-dimensional heat transfer calculation and stated that a two-dimensional analysis including fiber thickness should be performed. In scope of this study, a two-dimensional transient heat transfer analysis code is developed. The effect of parameters related to heat transfer during FDM, such as extrusion temperature, layer thickness, heating-cooling profile, production speed, substrate (base platform) surface temperature, should be examined.

Computational Methodology

Governing Equation and Discretization

Time-dependent heat diffusion equation is used to calculate transient temperature values inside a solid domain (Equation 4) (Bergman & Adrienne, 2017). Note that below equation assumes that conductivity of the material is constant and uniform.

$$\left| \frac{\partial^2 T}{\partial x^2} + \frac{\partial^2 T}{\partial y^2} + \frac{\partial^2 T}{\partial z^2} + \frac{q}{k} = \frac{\rho c_p}{k} \frac{\partial T}{\partial t} \right. \quad (4)$$

Here $x, y, z, T, \rho, c_p, q, k, t$ denotes x-coordinate, y-coordinate, z-coordinate, temperature, density of the polymer, specific heat of the polymer, volumetric heat generation rate, conductivity of the polymer and time, respectively.

Simplified version of this equation with no-heat generation assumption and two-dimensional approximation, the equation reduces to Equation 5:

$$\left| \frac{\partial^2 T}{\partial x^2} + \frac{\partial^2 T}{\partial y^2} = \frac{\rho c_p}{k} \frac{\partial T}{\partial t} \right. \quad (5)$$

With second-order central difference discretization in space, first-order backward difference in time, and implicit solution scheme, discretized form of the equation is obtained as follows:

$$\frac{T_{i-1,j}^n - 2T_{i,j}^n + T_{i+1,j}^n}{(\Delta x)^2} + \frac{T_{i,j-1}^n - 2T_{i,j}^n + T_{i,j+1}^n}{(\Delta y)^2} = \frac{\rho c_p}{k} \frac{T_{i,j}^n - T_{i,j}^{n-1}}{\Delta t} \quad (6)$$

Equation 6 contains i and j indices for the nodes representing discretization on x and y coordinates as shown in Figure 1. The superscripted index n denotes discretion in time. Δx , Δy and Δt are mesh sizes on x -direction, y -direction, and time.

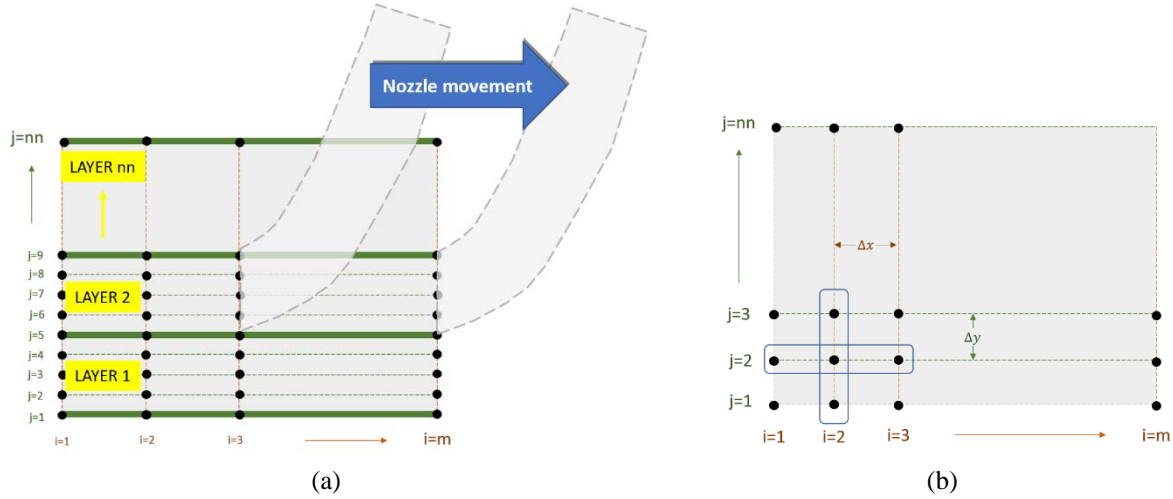


Figure 1. Domain and nozzle movement (a), Stencil of discretization (b)

With the help of the scheme in Equation 6 for discretization at all nodal locations, multiple equations are obtained. Total number of unknowns (nodal temperatures) are equal to the total number of equations and these equations constructs a matrix system. Note that coefficients of nodal temperatures at n^{th} time, so called a , b , c in Equation 4, and nodal temperature at $(n-1)^{\text{th}}$ time step are known values.

$$|a T_{i,j}^n + b T_{i-1,j}^n + b T_{i+1,j}^n + c T_{i,j-1}^n + c T_{i,j+1}^n = T_{i,j}^{n-1} \quad (7)$$

$$\begin{bmatrix} a & b & & & c & \cdot & c & & \\ b & a & b & & & & c & \cdot & c \\ & b & a & b & & & & c & \cdot \\ c & & & b & a & b & & & c \\ \cdot & c & & & b & a & b & & \\ c & \cdot & c & & \cdot & \cdot & \cdot & & \\ & \cdot & \cdot & \cdot & \cdot & \cdot & \cdot & & \\ & & c & \cdot & c & & b & a \end{bmatrix} \begin{bmatrix} T_{1,1}^n \\ T_{2,1}^n \\ T_{3,1}^n \\ \vdots \\ \vdots \\ \vdots \\ T_{m,nn}^n \end{bmatrix} = \begin{bmatrix} T_{1,1}^{n-1} \\ T_{2,1}^{n-1} \\ T_{3,1}^{n-1} \\ \vdots \\ \vdots \\ \vdots \\ T_{m,nn}^{n-1} \end{bmatrix} \quad (8)$$

Where $|a = (1 + 2Fo_x + 2Fo_y)$, $|b = -Fo_x$, $|c = -Fo_y$.

Dimensionless numbers in these coefficients are defined as $Fo_x = \frac{\alpha \Delta t}{(\Delta x)^2}$, $Fo_y = \frac{\alpha \Delta t}{(\Delta y)^2}$ where $\frac{k}{\rho c_p} = \alpha$.

The matrix system in Equation 8 has a form $A X = B$, where A is the coefficient matrix, X is unknown vector and B is known vector. Solving this matrix equation, nodal temperatures at n^{th} time are obtained by using the temperature values in the previous time step $(n-1)$. The calculation procedure starts with the utilization of initial temperature at $t=0$ sec as an initial condition and progresses until the end time of the simulation. In other words, by replacing the newly obtained X -vector with the B -vector, the solution advances in time (using $n=0$ as starting point for $n=1$, using $n=1$ for $n=2$, and so on).

The coefficient matrix (A) can be created with the help of a code and the matrix equation can be solved in a computer environment with the do-loops as marching in time. In scope of this study, a special code is developed by using Fortran 90 programming language to analyze heat transfer in a growing solid domain continuously changing boundaries and boundary conditions. In addition, the GMRES matrix solver (Turan & Eceder, 2011), which employs Newton-Krylov Method (Brown & Saad, 1989), is utilized to speed up the calculation process.

Initial and Boundary Conditions

The general representation of the applied boundary conditions is depicted in Figure 2.

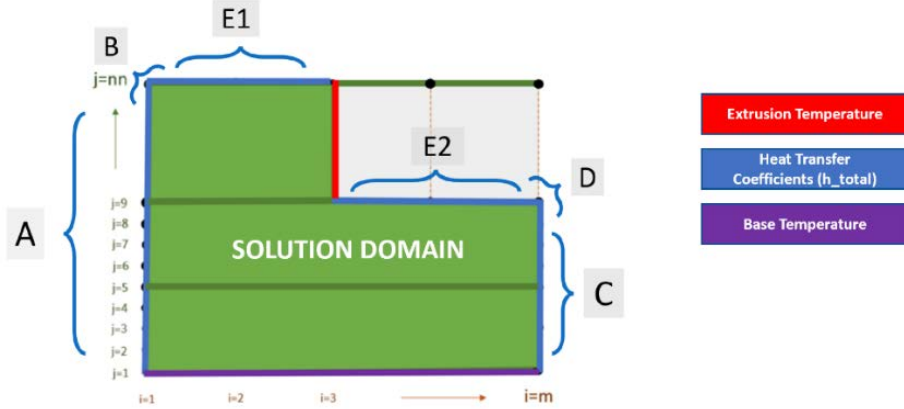


Figure 2. Boundary conditions

Blue lines in Figure 2, which consists of A, B, C, D, E1, E2 edges and corners, are subjected to an effective heat transfer coefficient that embodies convection and radiation heat transfer coefficients. After some algebraic manipulation, the concluding boundary equations are given in Table 1.

$$Q = h_{effective} A (T_{i,j}^n - T_{\infty}) \tag{9}$$

$$h_{effective} = h_{radiation} + h_{convection} \tag{10}$$

$$h_{radiation} = (T_{i,j}^{n-1} + T_{\infty}) [(T_{i,j}^{n-1}) + T_{\infty}^2] \tag{11}$$

$$Bi_x = \frac{h_{effective} \Delta x}{k} \tag{12}$$

$$Bi_y = \frac{h_{effective} \Delta y}{k} \tag{13}$$

Table 1. Equations at boundaries with heat transfer coefficients

1. A 2. Left Edge	3.
	4. $(2Fo_x + 2Fo_y + 2Bi_x Fo_x + 1)T_{i,j}^n - 2Fo_x T_{i+1,j}^n - Fo_y T_{i,j-1}^n - Fo_y T_{i,j+1}^n = 2Bi_x Fo_x T_{\infty} + T_{i,j}^{n-1}$
6. B 7. Top-Left Corner	5. 8.

		$9. \left\{ \frac{(2Fo_x + 2Fo_y + 2Bi_x Fo_x + 2Bi_y Fo_y + 1)T_{ij}^n - 2Fo_x T_{i+1,j}^n - 2Fo_y T_{i,j-1}^n}{10.} = 2Bi_x Fo_x T_\infty + 2Bi_y Fo_y T_\infty + T_{ij}^n \right.$
11. C 12. Right Edge		$14. \left\{ \frac{(2Fo_x + 2Fo_y + 2Bi_x Fo_x + 1)T_{ij}^n - 2Fo_x T_{i-1,j}^n - Fo_y T_{i,j-1}^n - Fo_y T_{i,j+1}^n}{15.} = 2Bi_x Fo_x T_\infty + T_{ij}^{n-1} \right.$
16. D 17. Top-Right Corner		$19. \left\{ \frac{(2Fo_x + 2Fo_y + 2Bi_x Fo_x + 2Bi_y Fo_y + 1)T_{ij}^n - 2Fo_x T_{i-1,j}^n - 2Fo_y T_{i,j-1}^n}{20.} = 2Bi_x Fo_x T_\infty + 2Bi_y Fo_y T_\infty + T_{ij}^n \right.$
21. E1 & E2 22. Top Edge		$24. \left\{ \frac{(2Fo_x + 2Fo_y + 2Bi_y Fo_y + 1)T_{ij}^n - Fo_x T_{i+1,j}^n - Fo_x T_{i-1,j}^n - 2Fo_y T_{i,j-1}^n}{25.} = 2Bi_y Fo_y T_\infty + T_{ij}^{n-1} \right.$

Note that radiative heat transfer coefficient is calculated by using the nodal temperature in previous time step.

In Figure 2, the extrusion temperature is shown as red line to define primary heat source. The boundary condition on this edge is applied as $T_{ij}^n = T_{extrusion}$. Same approach is employed for the base temperature, which is a constant value, $T_{ij}^n = T_{base}$.

Parameters for Preliminary Analysis

Assumptions:

- The temperature of the melted plastic coming from the nozzle is constant.
- Material properties are homogenous inside the solution domain.

Boundary Conditions:

- The extrusion temperature is equal to 210 °C.
- Base temperature is 60 °C.
- Air temperature is assumed to be 20 °C.
- The speed of nozzle (production speed) is 60 mm/s.

Material Properties:

Temperature-dependent material properties are used for the accurate calculation of matrix coefficients. Fitted equations to the property data provided in literature (Sin, Rahmat, & Rahman, 2012) are as follows:

- Conductivity (T in Kelvin), $k=0.130 \text{ W/m-K}$
- Specific Heat of PLA;
For $T > 330 \text{ K}$; $c_p \text{ (J/kg-K)} = 1.031698*T + 1677.2415$
For $T < 330 \text{ K}$; $c_p \text{ (J/kg-K)} = 3.969*T + 159.72$
- Density of PLA (T in Celsius);
 $\rho \text{ (kg/m}^3\text{)} = 1240 \text{ kg/m}^3$

The Geometry and Computational Parameters:

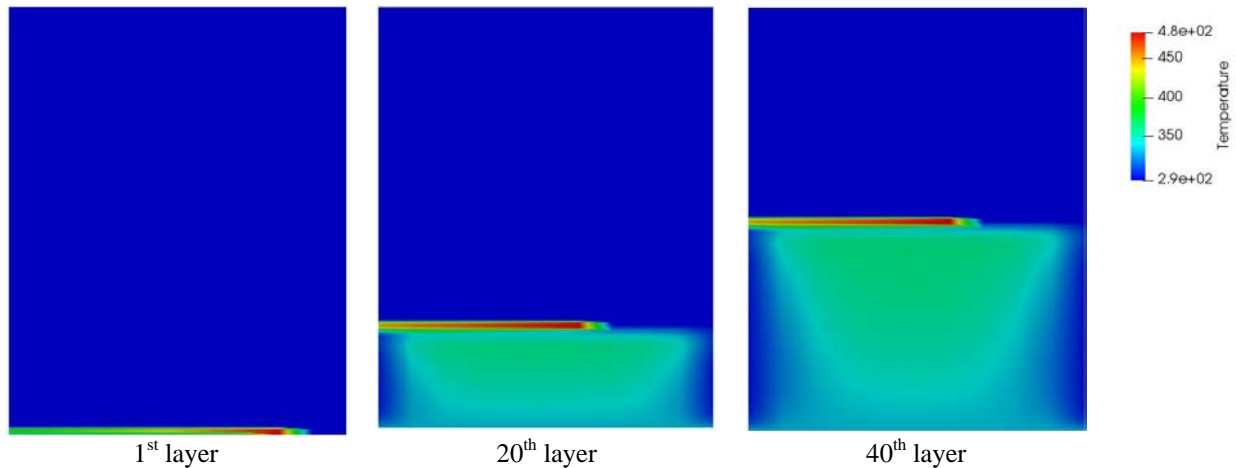
- X-direction: Width of the part is 19 mm, and it is divided into 10 segments ($\Delta x=1.9 \text{ mm}$).
- Y-direction: Layer thickness is 0.3 mm, and the total height is 25 mm which approximately corresponds to printing of 80 layers. Each layer (0.3 mm) is discretized by 3 nodes to resolve layer thickness ($\Delta y=0.10 \text{ mm}$).
- Time: The algorithm is designed to advance 1 node at every time step. The time step size, $\Delta t=\Delta x/\text{speed}$, is calculated as 0.03167 seconds.

Between consecutive layers, a time delay is defined to allow cooling process taking place during the production in third dimension. Intra-layer printing time is calculated with considering total area to be printed at each layer. With using the geometrical parameters, intra-layer delay is estimated as 3.8 seconds that corresponds to 120 time steps/layer. Following the completion of the printing process, an ultimate cooling time of 1,600 steps (~50 seconds between 10,280th and 11,880th time steps) is defined after the completion of the printing to observe cool down.

Results and Discussion

Preliminary Simulation Results

Preliminary results are obtained with the assumption that convective heat transfer coefficient is equal to $500 \text{ W/m}^2\text{-K}$ and $T_{\text{base}}=60 \text{ }^\circ\text{C}$. Contour plots in Figure 3 visualize temperature changes inside the printed part at different timesteps. Heat diffusion inside the domain, cooling effects from top, left and right boundaries are clearly observed. Thermal energy deposited during the printing process keeps layers above T_g at hotter locations. Note that T_g is between $50 \text{ }^\circ\text{C}$ and $80 \text{ }^\circ\text{C}$ for PLA (Matyjaszewski & Möller, 2012).



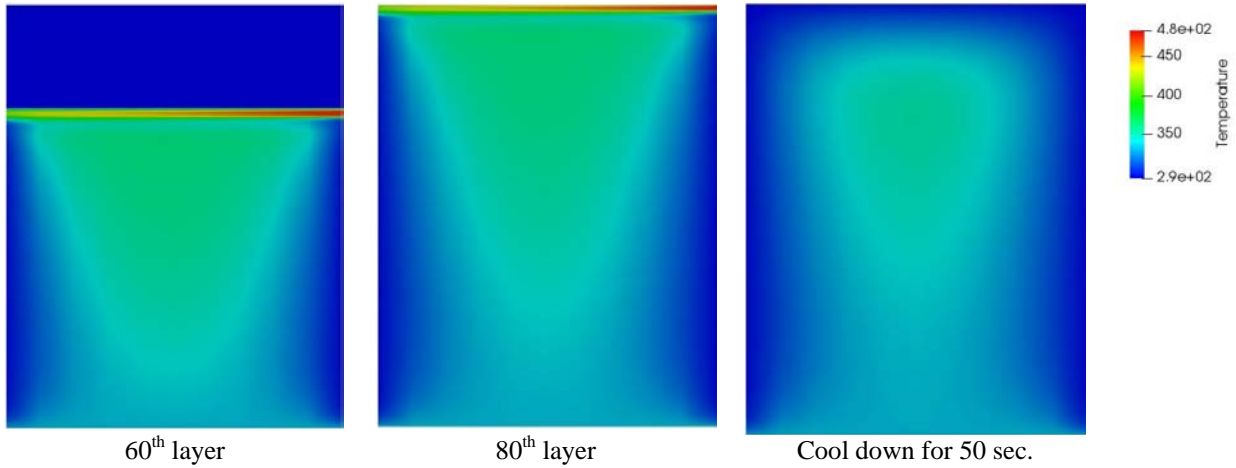


Figure 3. Computed temperature contour plots at different time steps (T in Kelvins)

Time history of nodal temperatures at the center of 2nd, 20th, 40th and 60th layers are given in Figure 4.

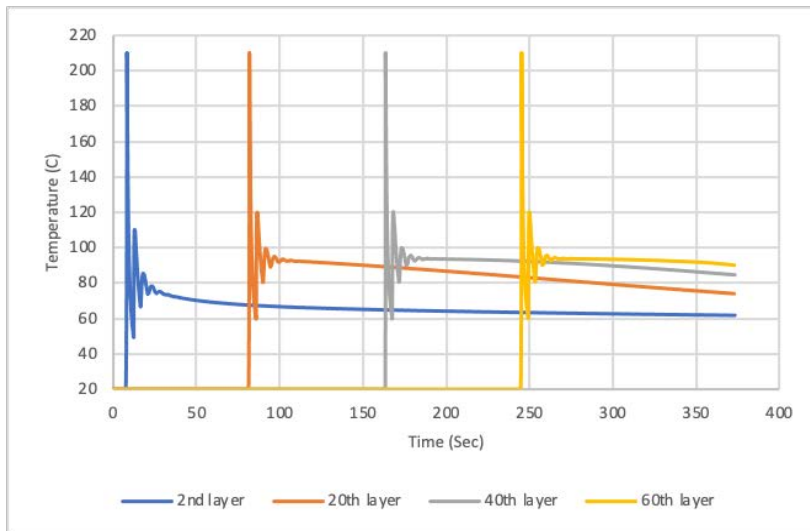


Figure 4. Nodal temperatures at the center node of layers

An experimental study in literature experimentally analyzed the effect of processing conditions on the bonding quality of FDM polymer filaments (Sun, Rizvi, Bellehumeur, & Gu, 2008). The time history of temperature data shows peaks with frequencies dependent on the printing speed and the printing path.

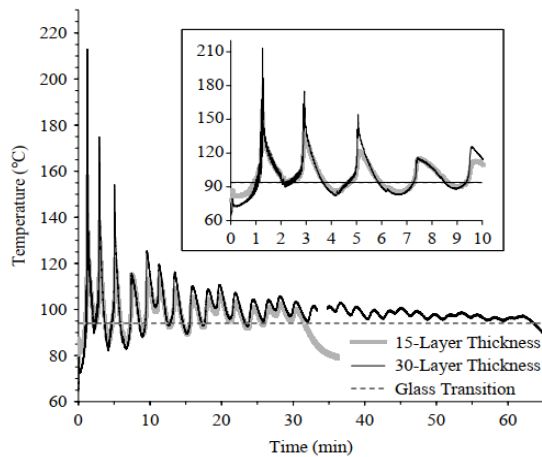


Figure 5. The time history of the measured temperature by k-type thermocouple during FDM (Sun, Rizvi, Bellehumeur, & Gu, 2008)

Conclusion

In scope of this study, a Fortran code is developed for the modeling of transient two-dimensional heat diffusion equation to understand history of temperature during 3D printing process via FDM. A matrix equation is obtained at each time step due to implicit time scheme which assures convergence of the solution regardless of the mesh size. The matrix is solved with the help of Newton-Krylov algorithm at each time step. A delay time is defined between layers and matrix is solved under convection and radiation boundary conditions at this time interval to consider the cool down period due to continuing extrusion process in the third dimension at the same layer.

During the simulation of the printing process, convection and radiation boundary conditions are applied to capture accurate cooling rate. $500 \text{ W/m}^2\text{-K}$ as the convective heat transfer coefficient (HTC) is applied to see the cooling pattern clearly. This number is the upper limit of the generic range of convection coefficients of air; $2.5\text{-}25 \text{ W/m}^2\text{-K}$ for natural convection, and $100\text{-}500 \text{ W/m}^2\text{-K}$ for forced convection (Kosky, Balmer, Keat, & Wise, 2013). It is important to remark that this elevated HTC intrinsically compensates lacking cooling effects in the third dimension which is expected to have the highest contribution to the overall heat transfer since front and back surfaces have relatively large areas compared to the other sides.

The two-dimensional code can be calibrated with the use of measured temperatures via infrared camera. Then, the calibrated code can be used for the estimation of t_{weld} , total welding time above glass temperature, at different production parameters. A $t_{\text{weld}}\text{-}\sigma$ correlation can be developed with tensile tests of the parts that are manufactured under corresponding production parameters. The authors continue to work tensile tests for the determination of a $t_{\text{weld}}\text{-}\sigma$ correlation for PLA.

Recommendations

As a future work, modeling of the third dimension with actual printing path is recommended. Convection from back and front surfaces contributes to cooling which has an impact on time history of temperatures. Further improvement of the code to include discretization of the third dimension may result in more accurate estimation of t_{weld} .

Scientific Ethics Declaration

The authors declare that the scientific ethical and legal responsibility of this article published in EPSTEM journal belongs to the authors.

Acknowledgements and Notes

* This article was presented as an oral presentation at the International Conference on Basic Sciences, Engineering and Technology (www.icbaset.net) conference held in Istanbul/Turkey on August 25-28, 2022.

* This research was supported by Simularge A.Ş. and its cloud infrastructure to run developed algorithms. We thank Dr. Erhan TURAN, CTO of Simularge A.Ş., for his insights that greatly assisted the research.

References

- Bartolai, J., Simpson, J., & Xie, R. (2018). Predicting strength of additively manufactured thermoplastic polymer parts produced using material extrusion. *Rapid Prototyping Journal*, 24(2), 321-332.
- Bergman, T. L., & Adrienne, L. S. (2017). *Fundamentals of Heat and Mass Transfer*. Wiley.
- Bikas, H., Stavropoulos, P., & Chryssolouris, G. (2016). Additive manufacturing methods and modelling approaches: a critical review. *Int. J. Adv. Manuf. Technology*, 83, 389-405.
- Coogan, T., & Kazmer, D. (2017). Bond and part strength in fused deposition modeling. *Rapid Prototyping Journal*, 23(2), 414-422.

- Coogan, T., & Kazmer, D. (2017). Healing simulation for bond strength prediction of FDM. *Rapid Prototyping Journal*, 23(3), 551-561.
- Faludi, J., Bayley, C., Boghal, S., & Iribarne, M. (2015). Comparing environmental impacts of additive manufacturing vs. traditional machining via life-cycle assessment. *Rapid Prototyping Journal*, 21(1), 14-33.
- Jud, K., Kausch, H., & Williams, J. (1981). Fracture mechanics studies of crack healing and welding polymers. *Journal of Materials Science*, 16(1), 204-210.
- Kosky, P., Balmer, R., Keat, W., & Wise, G. (2013). Mechanical engineering. In *Exploring Engineering - an Introduction to Engineering and Design* (p. 264). Academic Press.
- Matyjaszewski, K., & Möller, M. (2012). *Polymer science: a comprehensive reference*. Elsevier Science.
- Sin, L. T., Rahmat, A. R., & Rahman, W. W. (2012). *PLA handbook series: polylactic acid - pla biopolymer technology and applications*. Plastics Design Library.
- Sun, Q., Rizvi, G., Bellehumeur, C., & Gu, P. (2008). Effect of processing conditions on the bonding quality of FDM polymer filaments. *Rapid Prototyping Journal*, 14(2), 72-80.
- Turan, E., & Ecdar, A. (2011). Analysis of a bimetallic slab in non-isothermal flow. *Proceedings of the Institution of Mechanical Engineers, Part C: Journal of Mechanical Engineering Science*, 225(3), 658-672.
- Wool, R., & O'Connor, K. (1981). A theory of crack healing in polymers. *Journal of Applied Physics*, 52, 5953-5963.
- Yang, F., & Pitchumani, R. (2002). Healing of thermoplastic polymers at an interface under nonisothermal conditions. *Macromolecules*, 35, 3213-3224.

Author Information

Buryan Apacoglu-Turan

Istanbul Technical University
Faculty of Mechanical Engineering, Türkiye
Contact e-mail: apacoglu@itu.edu.tr

Kadir Kirkkopru

Istanbul Technical University
Faculty of Mechanical Engineering, Türkiye

To cite this article:

Apacoglu-Turan, B. & Kirkkopru, K. (2022). Development of two-dimensional thermal analysis code for the analysis of 3D printed PLA parts. *The Eurasia Proceedings of Science, Technology, Engineering & Mathematics (EPSTEM)*, 18, 28-36.